Laser ablation synthesis in solution and size manipulation of noble metal nanoparticles

Vincenzo Amendola* and Moreno Meneghetti

Received 15th January 2009, Accepted 24th February 2009
First published as an Advance Article on the web 1st April 2009
DOI: 10.1039/b900654k

In the past years, laser ablation synthesis in solution (LASiS) emerged as a reliable alternative to traditional chemical reduction methods for obtaining noble metal nanoparticles (NMNp). LASiS is a ''green'' technique for the synthesis of stable NMNp in water or in organic solvents, which does not need stabilizing molecules or other chemicals. The so obtained NMNp are highly available for further functionalization or can be used wherever unprotected metal nanoparticles are desired. Surface functionalization of NMNp can be monitored in real time by UV-visible spectroscopy of the plasmon resonance. However LASiS has some limitations in the size control of NMNp, which can be overcome by ''chemical free'' laser treatments of NMNp. In this paper we provide an overview of LASiS, size manipulation by laser irradiation and functionalization of NMNp, with special care in pointing out some of the main issues about this research area.

1. Introduction

In the wide panorama of nanomaterials, noble metal nanoparticles (NMNp) are attracting great interest due to their peculiar physical and chemical properties.[1,2] NMNp have at least one of the following distinctive features (Fig. 1): (i) the presence of optically active plasmonic modes which originate intense absorption and scattering bands in the visible–near infrared interval; the extinction cross-section of NMNp can be as high as 10^6 times that of the best organic chromophores;[1] the local field amplification due to plasmon resonances is also at the basis of surface enhanced Raman scattering (SERS);[3] (ii) the easy surface functionalization with a wide series of organic molecules; the metal–sulfur chemical bonds or the metal–amine physical bonds are usually exploited for the conjugation;[2] (iii) the chemical and physical stability and, in some cases, biocompatibility; depending on the metal, NMNp can resist high temperature, photoirradiation, acids or oxidation and no acute citotoxicity have been reported for NMNp;[1,2,4] important catalytic properties also derive from the chemical stability and surface chemistry of NMNp.[2,5,6]

NMNp appeared early in human history, probably since the 5th century BC in China and Egypt for medical or decorative purposes, which persisted until now.[2] Presently, NMNp are involved in various technological areas, like sensing, catalysis, electronics and plasmonics.[1,2] In particular, the use of noble metal nanostructures with plasmonic properties is rapidly increasing in biology and medicine.[1,2,4] Sensing of DNA and proteins[7] or the design of innovative tools for cancer therapy and diagnosis are some of the most promising topics.[8] Easy to guess as this rapid crossover from the field of nanosciences to

Department of Chemical Sciences, University of Padova, Via Marzolo 1, I-35131, Padova, Italy. E-mail: vincenzo.amendola@unipd.it

Vincenzo Amendola

Vincenzo Amendola (PhD in Material Science and Engineering, Padova) is Lecturer at the University of Padova at the Department of Chemical Sciences. His main interests are: LASiS of nanostructured materials, optical properties of NMNp; manipulation of shape, size and plasmonic features of nanoparticles by laser or chemical techniques; SERS and nonlinear optical properties of organic molecules supported on NMNp; functionalization strategies for application of NMNp in nanomedicine.

Moreno Meneghetti

Moreno Meneghetti is a Full Professor of Physical Chemistry at the University of Padova, Department of Chemical Sciences. His main interests are in linear and non linear interactions of electromagnetic radiation with molecular and nanostructured materials. He is now studying, also using a model approach, metal nanoparticles (synthesis and functionalization), carbon nanotubues (functionalization and characterization) for their intrinsic properties and for their applications in the bionano field, and organometallic molecules for their excited states multiphoton absorptions.

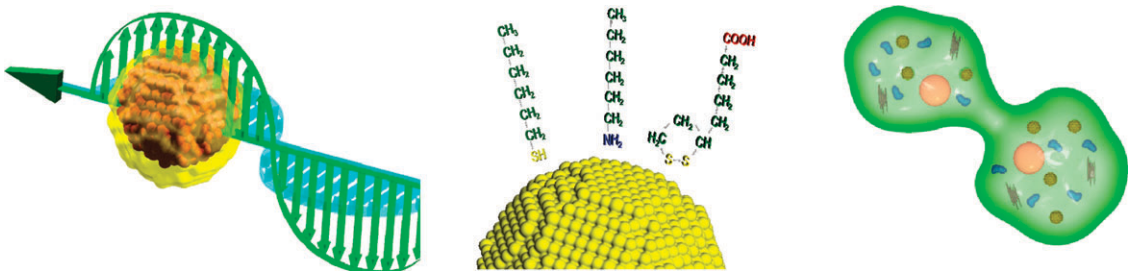

Fig. 1 Cartoons sketching three main peculiarities of NMNp: surface plasmon resonance; easy surface functionalization; chemical stability and *in vivo* biocompatibility.

the field of applied nanotechnology, nanobiotechnology and nanomedicine pushed to a refinement of NMNp synthetic techniques and *vice versa* in a virtual circle.[1,2]

The standard methods to obtain NMNp in solution consist in chemical reduction of metal salts in the presence of stabilizing molecules.[2] A large number of variants have been developed, corresponding to various combinations of metal precursors, solvents, reducing agents, stabilizing molecules, complexing agents and reaction conditions. Some of the most popular chemical reduction methods (CRMs) are: the citrate reduction method in aqueous solution, where citrate acts as both reducing and stabilizing agent; the $NaBH_4$ reduction method, which requires the presence of stabilizing agents in solution; the two phases Brust–Schiffrin method for obtaining thiols stabilized gold nanoparticles in organic solvents; the one phase reduction methods, which require metal precursors soluble in organic solvents and the presence of stabilizers.[2] Most variants to wet chemistry approaches are devoted to the synthesis of NMNp with a specific shape and structure,[1] which go beyond the scope of this paper. In general, CRMs offer several advantages, for instance the good control of particle size and shape and the versatility in the choice of solvents and ligands.[1,2] However, one can identify three principal classes of problems when dealing with NMNp obtained by CRMs (Fig. 2).

(i) Problems related to NMNp functionalization

Surface functionalization is at the basis of most applications of NMNp, because it confers specific functions such as solubility with long molecular chains, targeted delivery with biovectors, sensing with spectroscopic labels and so on. As a paradox, the addition of functional molecules in the synthesis environment before the reduction of metal salts, which is supposed to be the most intuitive way of obtaining functionalized NMNp, is also the less common option.[2,5,6] This is due to compatibility problems between functional molecules and reaction conditions but also to the sensitivity of CRMs to the properties of stabilizers, *i.e.* surface packing, bond strength and solubility.[2,5] Sometimes ligands bearing common reactive groups are used for NMNp synthesis and modified later by a subsequent chemical reaction with desired functionalities.[6,9–14] However, in case of thiols stabilized NMNp, ligand exchange reactions are the preferred strategy.[2,5,12] Such reactions are non-trivial and pose some limitations, as discussed in the perspective paper of Chechik and Caragheorgheopol.[5] First of all, not every type of thiolated molecule is suitable for place exchange reactions. For instance, the hindrance of incoming and outgoing thiols is a limiting parameter for the success of the place exchange reaction and it is arduous to make predictions about the extent of place exchange, therefore accurate analytical techniques are necessary to verify and quantify the extent of ligand exchange.[5] Moreover, the ligands around nanoparticles cannot be entirely replaced, the reaction speed is temperature dependent and heating is necessary to achieve the replacement in reasonable times, which is undesirable in case of thermosensitive molecules.[2,5] In case of citrate stabilized NMNp, the functionalization can occur in most cases by mixing molecules and nanoparticles, as citrate is weakly physisorbed on a metal surface and can be easily displaced from thiolated molecules.[2,15] However, the equilibrium of the colloidal system completely relies on adsorbed citrate molecules, and frequently particles aggregation happens during the functionalization process.[16–18] Moreover, a lower degree of surface functionalization was measured on citrate coated metal surfaces than on bare metal surfaces.[19]

(ii) Problems due to the presence of stabilizers on NMNp surface

In general, the presence of thiols, citrate or other ligands on the surface of nanoparticles can overshadow the role of the metal core when studying the physical–chemical interactions of NMNp with specific environments.[20–22] For instance, many thiols and disulfides were revealed as potentially toxic due to haemolytic effects.[23] Catalysis applications of NMNp also require highly accessible surface atoms and the absence of contaminations.[6,24] The same holds for energy or electron transfer in metal–semiconductor heterojunctions.[25,26] SERS usually requires the adsorption of molecules very close to the surface of metal particles having sizes on the order of tens of nanometers, which is difficult in case of thiolated nanoparticles.[3] Thiols have negative effects also on the plasmonic properties of NMNp. When a monolayer of thiols is present on the surface of gold and silver nanoparticles, an additional dumping of the surface plasmon band is observed, known as chemical interface dumping.[27] The extent of this dumping increases for decreasing the particles size, because it is a typical surface effect.[27,28] Therefore, a faster degradation of the plasmon resonance is observed in smaller nanoparticles.[28] This is a severe restriction when thiolated NMNp with plasmonic properties are desired, since the introduction of thiols in the synthesis environment pose limitations also on the maximum average size of NMNp, which usually lies below 5 nm.[2,5]

(iii) Problems due to sustainability and reproducibility of CRM

Sustainability and reproducibility of NMNp synthesis are two issues posed by the chemical synthetic approach. For NMNp to cross the boundary between science and applied technology, a key point is the availability of a sustainable preparation method.[29] In nanomaterial synthesis, sustainability basically coincides with the 12 principles of green chemistry.[29] CRMs induce some concerns about sustainability, as proven by the numerous efforts in researching effective purification techniques or environmentally friendly chemical reduction strategies.[16,30–38] Purification is an indispensable step of CRMs and is necessary for obtaining biocompatible NMNp, because many of the chemicals adopted for the synthesis are citotoxic.[4] Unfortunately, purification represents an important reason for the scarce sustainability of CRMs, due to the amount of time, energy and waste required.[29] As far as "green" methods are concerned, they usually produce nanoparticles in water, with a poor control of size and with a thick layer of chemisorbed stabilizers, which makes the subsequent functionalization difficult.[16,30–38] Anyway, even the most "green" chemical reduction method of noble metal nanoparticles poses a problem, *i.e.* metal salts used as precursors must be compatible with a sustainable synthesis.[16,29]

Another relevant feature of CRMs is that they represent a wide group of different synthetic procedures which change for different NMNp, instead of a unique synthetic approach which can address the demand of various types of NMNp. This unveils the fact that minor changes in the final product may require major changes in the CRM adopted and that reproducibility of NMNp synthesis is not easy.[2,5,29] Hence, literature offers a massive series of reports about the specific problem of preparing one specific type of NMNp having one specific surface stabilizing layer, size distribution, solubility properties, surface functionalization, *etc*.[2,11]

In summary, CRMs are not always the adequate choice for the preparation of NMNp and it would be worth having an alternative synthetic approach, in order to enhance the diffusion of NMNp amongst heterogeneous scientific communities and to foster even more the expansion of NMNp in applied technologies.

Laser ablation synthesis in solution (LASiS) can be an effective technique for obtaining NMNp. In the LASiS method, nanoparticles are produced during the condensation of a plasma plume formed by the laser ablation of a bulk metal plate dipped in a liquid solution. LASiS is usually considered a top–down physical approach, it is free of the usual disadvantages of chemical procedures and can be complementary to the bottom–up chemical methods for the production of NMNp. Moreover, LASiS has the potential of being a unique method for the synthesis of nanoparticles of different metals, with different surface coatings (if any) and in different solvents. Nanoparticles of gold, silver, platinum, copper and other materials have been obtained by LASiS in water and organic solvents through this one step, simple procedure. However the physics and chemistry of LASiS are non-trivial and still require further understanding. In sections 2 and 3, we discuss the basic mechanisms of LASiS and the main results which have been reported about LASiS of NMNp.

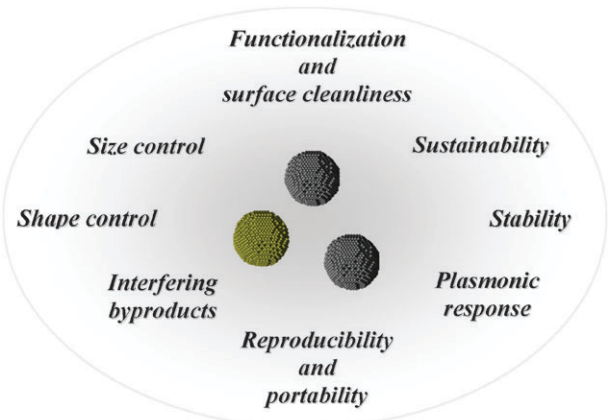

Fig. 2 Main issues concerning the synthesis of NMNp.

A major problem of LASiS is the control of NMNp size and size distribution, in particular when ligands-free nanoparticles are desired. However, the size of NMNp can be controlled by laser irradiation, exploiting plasmon absorption or interband transitions, without using chemical reagents. In section 4 we discuss the size manipulation of NMNp by laser irradiation.

On the other hand, a major advantage of LASiS is that NMNp can be obtained stable in water or organic solvents without stabilizing molecules or ligands. This provides great opportunities for particle functionalization through procedures easier than for NMNp obtained by CRMs. UV-visible spectroscopy of the surface plasmon absorption can be an effective method for real time monitoring of surface coverage during the addition of ligands. Some examples of functionalization of NMNp obtained by LASiS are reported and discussed in the last section of the paper.

To date, the physical aspects about LASiS of NMNp have been investigated more than the chemical ones. However, a comprehensive understanding of LASiS is still lacking and this means that such a technique has a large unrealised potential for the synthesis of NMNp and other nanostructures. For this reason, in the following of the paper our efforts have been devoted also in pointing out some of the issues about NMNp obtained by LASiS, in particular about the ablation processes, the stability and surface chemistry of NMNp, the size control of NMNp, the chemical reactions happening during the synthesis and, consequently, the opportunity of obtaining complex shapes or structures in reactive environments.

2. LASiS of NMNP: technical outline

Laser ablation is a well established technique in heterogeneous disciplines like surgery for the removal of tissues, mass spectrometry for the matrix assisted laser desorption ionization of samples, and thin film deposition by pulsed laser ablation of targets in ultra-high vacuum systems.[39] The application of laser ablation in liquids for the synthesis of nanomaterials is quite recent, since it has been pioneered by Henglein in 1993.[40]

Experimental set-up

The LASiS approach for the synthesis of NMNp has a strength point in the basic experimental set-up, which requires

a minimum manual operation. It consists in a pulsed laser, a set of focusing optics and a vessel containing the metal plate, which is placed in proximity of the focus (Fig. 3). The main start-up cost is represented by the laser, which can be quantified in *ca* 15 000 euros for a compact nanosecond instrument with an output energy appropriate for laser ablation (about tens of mJ pulse^{-1}). The focusing optics, the cells and the remaining equipment account for a few hundreds of euros.

Almost all scientists reported the utilization of a similar set-up, except for few minor details. Sometimes, systems for target rotation and magnetic stirring of the liquid solution are adopted during the ablation process. Usually, the metal plate is placed prior to the focus to prevent breakdown of the liquid, and typical laser spots on bulk metal can range from millimeters to microns. Relevant modifications to LASiS set-up were performed only in specific cases, as for laser ablation in supercritical fluids or for nanoparticles deposition on substrates.[41,42]

Time duration, wavelength and fluence of laser pulses are relevant parameters for laser ablation. Lasers with fs, ps or ns pulses at visible or near infrared wavelengths have been exploited for the LASiS of NMNp in a wide interval of fluences between few J cm^{-2} and thousands of J cm^{-2}.

When comparing LASiS to CRMs in view of the large scale or an industrial application, there are some aspects which need to be evaluated. On the one hand, LASiS has some limitations: (i) controlling the average size and size distribution of NMNp is difficult, as discussed in the following sections; (ii) the nanoparticles production rate, which is about 1–5 mg h^{-1} with a nanosecond laser, can be too low if mass production in short times is required; (iii) the start-up costs due to the laser and laser equipment can be excessive when a chemical laboratory is already present. On the other hand, LASiS requires: (i) minimum manual operation, which traduces in sensible time earnings for the operator; (ii) raw materials for the synthesis, which transduces to sensible money earnings for the purchase of metal plates instead of metal salts and other chemicals; (iii) minimum waste production during the synthesis procedure, which transduces to sensible money earnings for the disposal of hazardous or chemical waste produced by CRMs.

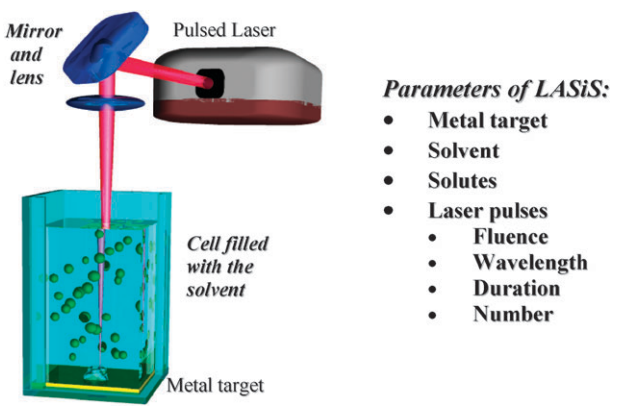

Fig. 3 The principal components of the experimental set-up for LASiS with a list of its main parameters.

Ablation mechanism

The current understanding of laser ablation is partly fragmented because of the complexity of the involved physical processes. Therefore making predictions about this phenomenon is a complex matter.[43–45] Laser ablation of a target starts with the absorption of incoming photons, which can produce the heating and photoionization of the irradiated area. Subsequently, some material can be torn away from the target as vapours, liquid drops, solid fragments or as an expanding plasma plume.[44–46] The phase and the amount of ablated material depend on the absorbed energy E.[43] The following trends have been estimated and measured for the ablation depth, L_a, the duration of the ablation process, τ_a, and the electronic temperature during the ablation process T_e:[43]

$$\text{for } \tau_a \gg \tau_l,\ L_a \propto E^{\frac{2}{3}},\ \tau_a \propto E^{\frac{1}{2}},\ \tau_e \propto E^{\frac{1}{3}}, \qquad (1)$$

where τ_l is the laser pulse duration. Usually, the production of about 1 mg of NMNp requires 10^5 laser pulses, corresponding to ablation times of the order of 20′ at 10 Hz (*i.e.* nanosecond or picosecond lasers) or of the order of 100″ at 1 KHz (*i.e.* femtosecond lasers). These figures suggest that LASiS can be suitable for mass production of NMNp only in the latter case.

Several authors reported that a satisfactory ablation rate can be obtained when the absorbed energy is high enough to produce a plasma plume. During LASiS of NMNp, the formation of a plasma plume can be observed through emission of light and is accompanied by a sound wave.[47,48] During laser ablation in liquids, the plasma plume is effectively confined near the target by the liquid buffer, which has implications in the ablation yield of the metal target.[45,47,48] In fact, the target faces the plasma plume at high temperature and pressure for a time long enough to be ablated by the plume even after the end of the laser pulse.[45,47–49] Spectroscopic studies with streak CCD cameras measured a decay time of several tens of nanoseconds for a plasma plume obtained through laser irradiation of metal targets in water with 20 ns–1064 nm pulses at various fluences.[47] However also boiling, vaporization and explosive processes are observed simultaneously to the plasma formation. In fact, the profile of absorbed energy is non-constant in time and non-uniform on the whole target area,[45,50,51] which is one of the reasons for the quite large size distributions of NMNp obtained by LASiS.[51] Also, the charging of the irradiated area due to photoionization contributes to the expulsion of material from the target.[52] Due to the coexistence of these different processes, the ablation mechanism of LASiS is sometimes defined as "explosive boiling" or "explosive ablation" mechanism.[44,45,50]

The phase homogeneity of the material detached by laser ablation is a main issue of LASiS, because it has implications in size, size distribution, surface and inner composition of nanoparticles. One can identify two different ablation regimes observing the morphology of craters in the target, which are correlated to the phase homogeneity of ablated material. Koshizaki and coworkers observed that 355 nm nanoseconds laser pulses with fluences in the range 5–50 mJ cm^{-2} produced

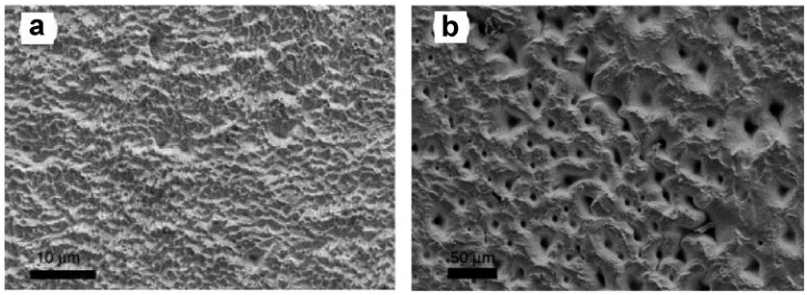

Fig. 4 SEM images of platinum targets after ablation at 355 nm wavelength for 15 min at 14 J cm^{-2} (a) and at 1064 nm wavelength for 15 min at 42 J cm^{-2} (b). Reprinted with permission from ref. 51. Copyright (2006) American Institute of Physics.

a homogeneous erosion of a Pt target, while 1064 nm nanoseconds laser pulses at same fluence produced a series of distinct micrometric craters in the whole irradiated area, corresponding to hot spots due to absorbing impurities (Fig. 4).[50] Laser irradiation with higher fluences determined a similar morphology, consisting in rugged craters, both at 355 and 1064 nm.[50] Kabashin and coworkers observed remarkable changes of morphology in the craters obtained in a gold plate by 110 fs–800 nm laser pulses at different fluences.[53] Fluence of 60 J cm^{-2} produced sharp craters, while 1000 J cm^{-2} produced irregular craters.[53] Both authors associated the different morphologies to different ablation mechanisms and observed the production of nanoparticles with different average size and size distribution.[51,53] Regular craters and low fluences were associated to NMNp with small average diameters (3–6 nm) and ascribed to the vaporization of the target.[51,53] Irregular craters and high fluences were associated to larger nanoparticles, having a size distribution peaked at tens of nanometers, ascribed to the explosive boiling of the target.[51,53]

Duration of laser pulses is an important parameter for LASiS. Femtosecond laser pulses release energy to electrons in the target on a time-scale much faster than electron–phonon thermalization processes, while picosecond and nanosecond laser pulses release energy on a time-scale comparable with the thermal relaxation processes of the target.[43,54] Consequently, some differences can be observed in the ablation mechanism with pulses of different length. By irradiation of organic microcrystals suspended in water, Asahi and coworkers observed photothermal or photomechanical ablation mechanisms with nanosecond or femtosecond laser pulses, respectively.[55] Moreover, experimental and theoretical studies evidenced that the ablation starts a few tens of picoseconds after the laser irradiation and that the plasma lasts for tens of nanoseconds.[43,45,47,53] In the case of nanosecond pulses, the plasma is present for a time roughly equal to twice the pulse duration.[45,47] Therefore, in the case of laser ablation with femtosecond or picosecond laser pulses, there is no temporal overlap between the pulses and the ejected material, which comes prevalently from the irradiated area.[43] On the contrary, in the case of LASiS with nanosecond pulses, there is an overlap with the ablated material and the ablation can also occur in a region larger than the irradiated area due to heat conduction.[43] The implications of the temporal overlap between laser pulses and the ablated material are important for the ablation mechanism. Molecular dynamics simulations and experimental measurements showed that high intensity laser pulses produced an expanding plume composed by a mixture of ionized atoms, clusters and larger fragments like liquid drops.[44,47] In the presence of a long laser pulse, the plasma plume can absorb part of the incoming laser energy, which further increases the temperature of the plasma and favours the atomization of the material contained in the plume.[45,47] This process can homogenize the phase of the material ejected from the target.[45,47] On the other hand, the laser energy absorbed by the target decreases due to the optical shielding of the plasma plume, while target ablation by interaction with the plasma plume is enhanced due to the increased plasma temperature.[45] The influence of such a process on the LASiS of NMNp and their competing or complementary function in the ablation mechanism need to be elucidated through deeper investigations.

The absorption cross-section of bulk metals is increased for decreasing laser wavelengths.[50] However, due to reabsorption effects, the irradiation at short wavelengths does not necessarily coincide with an increased ablation efficiency. Some NMNp have plasmon resonances or interband transitions in the UV-visible interval, therefore incoming laser pulses can be reabsorbed by freshly formed nanoparticles, with the double negative effects of decreasing the ablation rate and broadening the size distribution *via* photoinduced fragmentation.[56] Moreover, laser pulses at short wavelengths are efficiently absorbed by the plasma plume produced during the ablation process.[45] These phenomena introduce nonlinearity between the ablation efficiency and the absorption coefficient or the laser fluence. The use of near-infrared laser wavelengths can minimize the reabsorption effects.[56]

Nanoparticles formation

The prevailing formation mechanism of NMNp obtained by LASiS consists in nucleation during the plasma plume cooling followed by nuclei growth and coalescence (Fig. 5).[45,57] Three experimental findings support this observation. First, transmission electron microscopy (TEM) analysis evidenced the polycrystalline structure of NMNp obtained by LASiS.[58–60] Second, nanoparticles obtained by LASiS in the presence of ligands or stabilizing agents have a smaller average size with respect to particles obtained in pure solvents.[56,57] Third, LASiS in reactive solvents did not originate pure metal nanoparticles.[61]

The driving force for the nucleation of metal embryos in the plasma plume is the supersaturation, given by the ratio

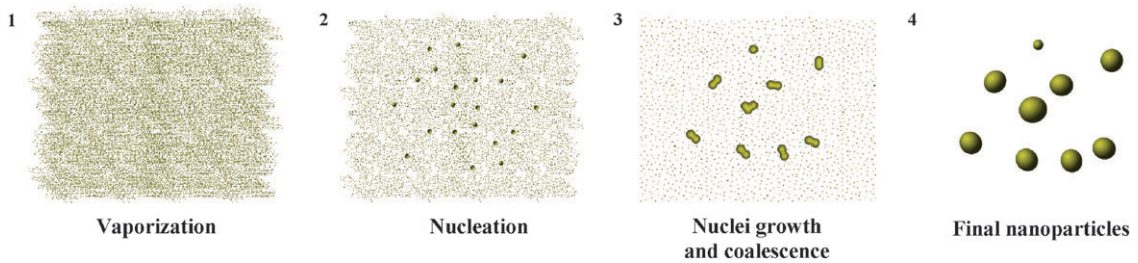

Fig. 5 Cartoon representing the stages of NMNp formation by LASiS.

between the actual vapour pressure p to the equilibrium vapour pressure $p_0(T)$ at the system temperature T.[45] The free energy barrier ΔG_N and the minimum radius R_N depend on the supersaturation $p/p_0(T)$ as:[45]

$$\Delta G_N \propto \left[k_B T \ln\left[\frac{p}{p_0(T)}\right]\right]^{-2}, \qquad R_N \propto \left[k_B T \ln\left[\frac{p}{p_0(T)}\right]\right]^{-1}, \tag{2}$$

where k_B is the Boltzmann constant. The nucleation process is fast and is followed by a diffusion limited growth process of the nuclei, which continue for hundreds of nanoseconds after the laser pulse.[45,56,57] During the growth, free metal atoms condense on nuclei and nuclei can also coalesce together, originating the typical polycrystalline structure of NMNp obtained by LASiS.[45,56,57] Mafuné and coworkers observed that the growth of ligand-free nanoparticles can continue for several days after the synthesis, because metal ions can last in solution for a long time after the formation of the plasma plume in the case of high affinity with the solvent, as for Pt and Ag in water.[57,62]

According to the above formation mechanism, the size of NMNp depends prevalently on the density of metal atoms during the nucleation and growth processes and on the temperature.[45,57] Unfortunately, the atomic density and the temperature profiles are not homogeneous everywhere in the plasma plume, since two boundary regions exist with the surrounding liquid and the metal target.[45,47] Moreover, the expansion of the plasma plume in the liquid buffer produces a concentration gradient of atomic and molecular species of the solvent, which is complementary to the concentration gradient of metal atoms.[45,47] During the plasma plume expansion, several species can participate in chemical reactions (Fig. 6), which are related to the concentration, pressure and temperature gradients.[45] The mixed layer containing metal and solvent excited species can favour chemical reactions even in the case of noble metals and stable solvents like water. Koshizaki and coworkers observed the prevailing formation of platinum hydroxides below a threshold of 4 J cm^{-2}, during LASiS experiments with 355 nm–7 ns pulses on a Pt target in water.[51,63] Several authors reported that an energy threshold exists for the LASiS of NMNp.[49,51,53,56,57] The fact that LASiS requires the presence of a plasma plume and has a fluence threshold for particles formation can be read as the need of a minimum metal atoms density in the ablated material for obtaining nanoparticles instead of side reactions with the solvent.[50,51,56,57]

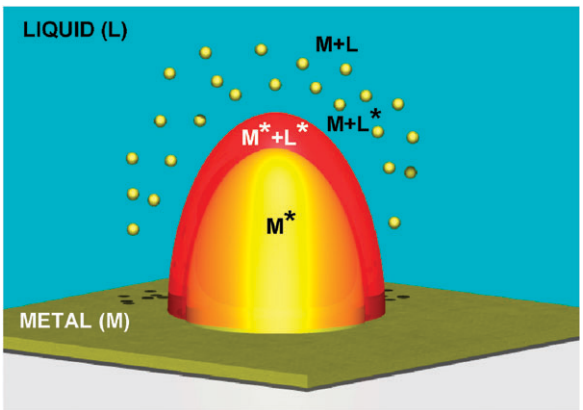

Fig. 6 Sketch of the plasma plume formed by laser ablation of a metal target. Four combinations of liquid and metal species can be identified due to different temperature, pressure and composition. The * denotes excited and/or ionized states.

Other indications of the interaction between ablated material and solvent were found by Koshizaki *et al.* with LASiS at high fluence (110 J cm^{-2}) with the Pt target placed below the focus.[63] This is an unusual focusing configuration because the laser beam produced the breakdown of water and the so obtained plasma was used for etching the Pt target. In this configuration, mixtures of Pt hydroxides with minor fractions of Pt nanoparticles were obtained.[63] Moreover, the observation by scanning electron microscopy of the Pt targets after ablation at 355 nm–7 ns pulses at fluences between 4 and 60 J cm^{-2} revealed the presence of a homogeneous surface patterning which was attributed to a spinodal decomposition at the molten target interface.[50]

The evidences of strong reactivity between metal and solvent in the plasma plume are consequences of the extreme pressure and temperature conditions.[45] On the other hand, the plasma plume is quenched one order of magnitude faster in liquids than in gas or vacuum and the cooling process may not be considered an adiabatic process.[45,64] This is useful for out-of-equilibrium reactions and the synthesis of metastable phases formed at high pressures and temperatures.[45]

Nucleation and growth do not represent the only formation mechanism of nanoparticles. In the previous subsection we anticipated, as Meunier and Koshizaki reported, the observation of a bimodal particle size distribution obtained by LASiS with femtosecond and nanosecond laser pulses and found that the relative weight of the two populations was dependent on the laser fluence.[51,53] They hypothesized that a secondary mechanism consisting in the ejection of melted drops or solid

fragments from the target (explosive boiling) was responsible for the fraction of larger nanoparticles.[51,53] However, direct confirmation of this mechanism is not provided in literature, although it can involve interesting implications, as in the case of LASiS in reactive environments for obtaining core@shell structures, because solid fragments and liquid drops should preserve cores of pure metal.[50]

The above formation mechanism implies that NMNp obtained by LASiS has a spherical or roughly spherical shape. Deviations from spherical symmetry are frequently observed in a minor fraction of particles, as a result of embryos coalescence soon after the nucleation process.[59,65] LASiS has never been used for obtaining well defined non-spherical shapes, except when particle aggregation into fractal structures occurs.[42]

3. LASiS of NMNp: results

Literature about LASiS of NMNp is quite large, although only a minor part reports deep investigations of the technique. The type of metal, of solvent, the presence of solutes or stabilizers and laser parameters like wavelength, time duration and fluence have been investigated. Several authors also studied the application of LASiS for the synthesis of semiconductor (Si, CdS, ZnSe, ZnO),[66–69] oxide (FeO),[70] sulfide (Hf_3S),[71] magnetic (Co),[72] organic nanoparticles[55] and metastable phases compatible with high temperatures and pressures (diamond, boron nitride, carbon nitride),[45] with interesting results in most cases.

Laser ablation in pure solvents is the simplest case of LASiS and ligand-free nanoparticles have a wider range of applications than ligand-coated NMNp. Therefore we consider NMNp obtained in pure solvents first and then we discuss the special case of NMNp obtained in the presence of stabilizing agents and other solutes.

LASiS in pure solvents

As summarized in Table 1, platinum, gold, silver and copper nanoparticles have been obtained by LASiS in a series of pure solvents by different laser pulses and with variable results in terms of average size and size distribution.

TEM analysis and UV-visible spectroscopy are usually exploited for obtaining information on synthesis results. TEM analysis show that the large part of NMNp obtained by LASiS have average sizes of 3–30 nm. Nanoparticles prevalently have a spherical shape, although spheroidal or irregular forms are frequent. The structure of NMNp is highly defective and often polycrystalline (Fig. 7), which is typical of the formation mechanism and the fast cooling described in the previous section.[58,59,65,73] UV-visible spectroscopy can be a fast technique for the characterization of particle shape and size in case of silver, gold and copper nanoparticles, which have a plasmon resonance. In general, the presence of a sharp plasmon band close to 400, 530 and 600 nm for Ag, Au and Cu is the proof that nanometric metallic nanoparticles with a spherical shape have been obtained by LASiS (Fig. 8).[27] The Mie model for spherical NMNp can provide information on particle size by fitting the experimental spectra.[27] However, the model is often ineffective in reproducing the plasmon extinction measured at wavelengths longer than the plasmon peak.[28,65] In that range a contribution to the overall plasmon band can be originated by nanoparticles with a nonspherical shape or aggregated due to the absence of stabilizing agents.[28,65] TEM analysis gives an indication of nonspherical shapes, while it is usually unreliable for the evaluation of the fraction of aggregated particles.[28,65] Recently we developed a procedure based on the fitting of the UV-visible spectra with the Mie and Gans models for the evaluation of gold nanoparticles' size with an accuracy of *ca* 6% and for the estimation of particles' concentration and of the fraction of nonspherical or aggregated nanoparticles (Fig. 9). The fitting program can be downloaded freely from the web (see ref. 28) and can, in principle, be also applied to AgNP and CuNP.

The control of size distribution and of the stability of the colloidal system are two main issues of NMNp obtained by LASiS in pure solvents. Unfortunately, the identification of important parameters for the control of particle size and stability is quite difficult due to the heterogeneity of the experimental conditions present in literature.

Larger average size and size distribution of NMNp are usually obtained with higher laser fluences, except when laser wavelength can be reabsorbed by nanoparticles, producing photofragmentation.[51,53,74] Short laser pulses are sometimes associated with very large average sizes and size distributions (see Table 1). The reason could be in the absence of interactions between the plasma plume and the same incoming laser pulse originating the plume, which is possible only with long pulses. Also the occurrence of explosive boiling or other photomechanical ablation mechanisms should be considered when using femtosecond pulses instead of nanosecond pulses with the same fluence.

No clear variations in the size distribution of NMNp were observed changing the metal type, except when differences in the plasmon resonance originated reabsorption effects. However, a trend is observed when comparing the size of NMNp obtained in water or in organic solvents. Sizes of about 10–40 nm are typical of nanoparticles obtained in water, while sizes of about 5–15 nm are observed for NMNp in organic solvents. The reason could be in different thermal properties of water with respect to all other organic solvents or in a strong interaction of organic solvents with the surface of NMNp, which is competitive with particle growth. The results of LASiS of AuNP in toluene show that the second hypothesis should be considered.[75] In the case of toluene, metal nanoparticles obtained by laser ablation are embedded in a solid matrix due to solvent pyrolysis consisting in a mixture of graphite nanocrystals and amorphous carbon (Fig. 10).[75] The average size of AuNP is 1.8 nm, much smaller than particles obtained in other solvents, which suggests that the matrix prevented further growth of nanocrystals. The matrix also quenched the plasmon band of AuNP.[75]

Pyrolysis is a remarkable drawback of laser ablation synthesis of NMNp in the presence of organic compounds, as it can virtually affect biocompatibility, stability and surface accessibility of NMNp. One can expect that pyrolysis is dependent on solvent reactivity at high temperatures, but also the metal type influenced the process. Good stability was observed by TEM and UV-visible analysis for AuNP and

Table 1 NMNp obtained by LASiS in pure solvents

Metal	Solvent	Size (standard deviation)	Pulse wavelength (duration) fluence	Ref.
Au	Water	18 nm (64%)	1064 nm (9 ns) 10–20 J cm^{-2}	61
	Water	4–130 nm	800 nm (120 fs) 60–1000 J cm^{-2}	50,54
	Water	11 nm	532 nm (5 ns) 4 J cm^{-2}	104
	n-hexane	10 nm (60%)	532 nm (5 ns) 1–200 J cm^{-2}	60
	Decane	5–8 nm	532 nm (5 ns) 4 J cm^{-2}	74
	Dimethylsulfoxide	4.8 nm (38%)	1064 nm (9 ns) 1–5 J cm^{-2}	66
	Tetrahydrofuran	8.2 nm (61%)	1064 nm (9 ns) 1–5 J cm^{-2}	”
	Acetonitrile	3.6 nm (67%)	1064 nm (9 ns) 1–5 J cm^{-2}	”
	Toluene	1.8 nm (55%)	1064 nm (9 ns) 3 J cm^{-2}	75
	Supercritical CO_2	500–30 nm	532 nm (9 ns) 0.8 J cm^{-2}	44
Ag	Water	11.4 nm	532 nm (5 ns) 4 J cm^{-2}	104
	Water	18 nm (50%)	1064 nm (ns)	Tsuji *et al.*; Appl. Surf. Sci. 2008, 5224
	Dimethylsulfoxide	7.8 nm (49%)	1064 nm (9 ns) 10 J cm^{-2}	59
	Tetrahydrofuran	4.8 nm (46%)	1064 nm (9 ns) 10 J cm^{-2}	”
	N,N-dimethylformamide	4.4 nm (114%)	1064 nm (9 ns) 10 J cm^{-2}	”
	Acetonitrile	3.8 nm (79%)	1064 nm (9 ns) 10 J cm^{-2}	”
Cu	Water	30 nm (47%)	1064 nm (10 ns)	79
	Acetone	3 nm (43%)	1064 nm (10 ns)	”
Pt	Water	3–6 nm	1064 nm (10 ns) 10–60 J cm^{-2}	52
	Water	3–6 nm	532 nm (8 ns) 10–60 J cm^{-2}	”
	Water	3–7 nm	355 nm (7 ns) 10–60 J cm^{-2}	”
	Water	6.2 nm (23%)	532 nm (ns)	Mafuné *et al.*; J. Phys. Chem. B 2003, 4218

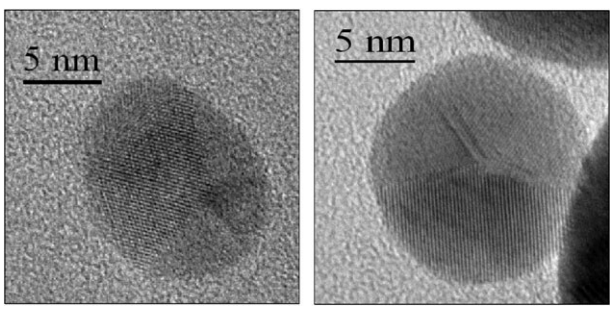

Fig. 7 HRTEM images of AgNP (left) and AuNP (right) obtained by LASiS in dimethylformamide and water, respectively. Both show a polycrystalline structure typical of metal nanoparticles obtained by LASiS.

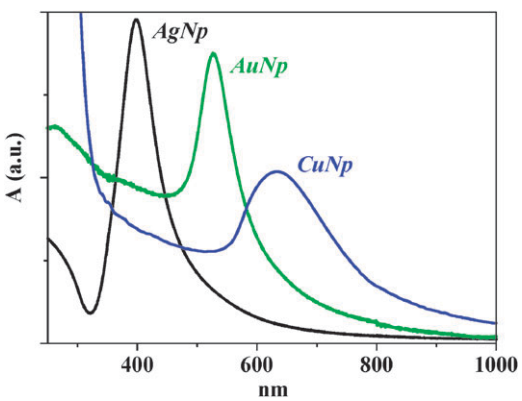

Fig. 8 Typical UV-visible spectra of Ag, Au and Cu nanoparticles obtained by LASiS. The prevalently spherical shape and size on the order of 2–40 nm originate a single sharp plasmon absorption at distinctive wavelengths for each metal.

AgNP in ethanol and other aliphatic alcohols, acetonitrile, dimethylformamide and acetone, while dimethylsulfoxide and tetrahydrofuran were revealed as good solvents for gold but not for silver.[58,59,61,65] However, the studies about pyrolysis during laser ablation in the presence of organic compounds are infrequent in literature and several points are still unexplored. For instance, it is not clear if oxygen plays a role in solvent degradation and, most important, if the products of solvent pyrolysis can adsorb on the NMNp surface, can adsorb on the bulk metal target or can be solubilized in the solvent. Also, the role of pyrolysis byproducts on the stability of colloidal NMNp solutions needs to be elucidated. However, the results of our group[58,65] and of Compagnini's group[59,61] showed that NMNp obtained in most organic solvents have lower time stability and higher propensity to aggregation than in water.

Nanoparticles stability is a crucial aspect of LASiS in pure solvents. Despite the absence of stabilizers, NMNp obtained in water and in several organic solvents are stable for days, months or even longer.[58,60,65] However, a fraction of aggregated or nonspherical nanoparticles is often present in NMNp solutions obtained by LASiS, as studied by UV-visible spectroscopy.[28,65] One can discriminate between two types of aggregation corresponding to two different mechanisms: (i) constant aggregation; and (ii) dynamic aggregation. Constant aggregation is often observed in AuNP obtained by LASiS in pure water, because UV-visible spectroscopy and Mie-Gans models evidenced a non-negligible fraction of nanoparticles with a nonspherical shape, as discussed above. However, this fraction of aggregated or nonspherical nanoparticles tends to be constant for months or even for years, hence suggesting that it is a product of LASiS and not of aggregation following the synthesis.[28] Dynamic aggregation is always observed in AuNP obtained by LASiS in pure organic solvents[65] and is due to particle instability on the time-scale of hours or weeks, depending on solvent type and particle concentration.

The use of NMNp obtained in the absence of stabilising agents should always consider the stability time frame for each set of metal nanoparticles and solvent. In the case of particle

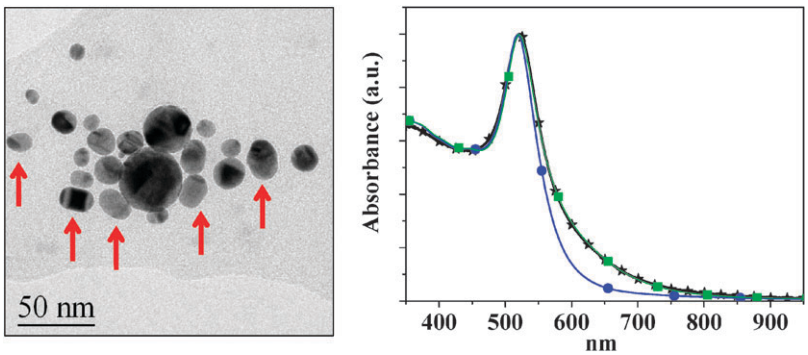

Fig. 9 Left: TEM image of AuNP obtained by LASiS in water. The arrows are indicating particles with a neat spheroidal shape. Right: Experimental UV-visible spectrum of AuNP obtained in water by LASiS (stars) and fitting with the Mie model for spherical particles (circles) and the Mie-Gans model for spherical and spheroidal particles (squares).

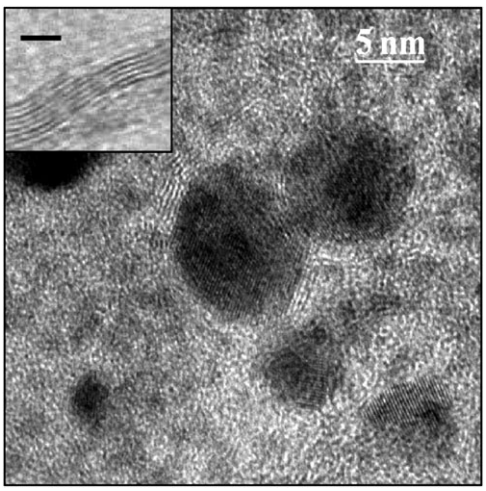

Fig. 10 TEM images of AuNP obtained by LASiS in toluene. In some cases, AuNP are surrounded by graphitic nanostructures. Inset shows a magnification of graphitic nanostructures, where the interplanar distance of 0.34 nm has been measured (bar = 2 nm). From ref. 75.

deposition on surfaces, stabilizers are required in order to avoid aggregation upon solvent drying.

Solvent purity is considered a prerequisite for obtaining stable colloidal solutions, although current knowledge about the surface chemistry of ligand-free NMNp is limited. In the absence of ligands, surface charges provide stability to nanoparticles obtained by LASiS in pure solvents. Z spectroscopy and electrophoresis experiments showed that AuNP obtained by LASiS in water have a negative charge.[76,77] However, the groups of Meunier and Mafuné found by X-ray photoelectron spectroscopy that a fraction of gold atoms was present with an oxidation state of +1 and +3.[76,77] These findings are in fair agreement with a recent report of Cuenya *et al.* about the surface oxidation of gold nanoparticles in the presence of O_2.[78] Also supported by FTIR and secondary ion mass spectrometry, Meunier and coworkers hypothesized that negative charges derive from the presence of Au–O^- species on a gold nanoparticle surface.[76,77] According to the results of Koshizaki *et al.* about LASiS of Pt, gold oxidation can happen as a consequence of the highly reactive plasma environment.[63,76,77] Mafune and co. estimated that about 3–7% of surface gold atoms owned a negative charge by a titration with a cationic surfactant like cethyltrimethyl ammonium bromide (CTAB).[76,77] Meunier and co. found that the pH of the solution influences the Z potential of AuNP probably through the equilibrium between Au–OH and Au–O^- species.[76,77] Koshizaki found that the pH of the solution was quite unchanged after the laser ablation,[63] which confirmed the result of Mafuné and co. that only a low percentage of surface atoms are oxidised.[76,77]

In the case of copper nanoparticles obtained by LASiS in water, evidences of the formation of copper oxides(II) were found also by UV-visible spectroscopy and X ray diffraction.[79,80] On the contrary, laser ablation of copper in acetone and of CuO powders in 2-propanol gave metallic CuNP.[79,81] These findings can be read as the proof that water is directly involved in the surface oxidation of NMNp, or, on the other hand, as an indication that organic solvents may have a capping effect on the surface of metallic nanoparticles preventing air oxidation. However the studies about LASiS of CuNp are less numerous than about other NMNp, therefore further investigations can help in elucidating their oxidation properties.

One can expect that silver nanoparticles undergo to surface oxidation at an intermediate level between gold and copper. Park and co. reported that AgNP showed a sharper plasmon band when obtained by LASiS in solutions containing Cl^- 5 mM than in pure water.[82] Analogous results were found by Meunier and co. for AuNP in a 1 mM NaCl and in NaOH (pH 9.4) aqueous solutions.[76,77] These results can be interpreted as a proof of surface oxidation, since it is supposed that Cl^- and OH^- ions are involved in the following reactions on the surface of nanoparticles:[76,77]

$$\text{Au–O–Au} + Cl^- \Rightarrow \text{Au–}O^- + \text{Au–Cl}$$
$$\text{Au–O–Au} + OH^- \Rightarrow \text{Au–}O^- + \text{Au–OH}.$$

Hence Cl^- and OH^- can produce a neat charge on particles surface, which prevented particles aggregation and the broadening of plasmon bands in the experiments of Meunier and Park.[77,82] Consequently, the presence of salts traces in pure solvents can be of paramount importance for the stability of NMNp obtained by LASiS. Controlling the surface chemistry and the stability of nanoparticles obtained by LASiS in pure solvents is, therefore, more complicated of what one can expect, since they can depend, for instance, on impurities,

solubilized atmospheric gases and pH variations due to absorbed CO_2.[77,82,83]

LASiS in presence of solutes

The effects of electrolytes, surfactants and thiolated ligands have been frequently studied in literature (Table 2), with the main objective of controlling particles size and size distribution or improving particles stability, with the consequent reduction of particles aggregation.

In general, the presence of electrolytes during LASiS has negative effects on the stability of NMNp, due to the screening of particles surface charge.[77,82,83] However, as discussed in the previous subsection, several authors reported enhanced ablation efficiency and nanoparticles stability by LASiS in aqueous solutions containing Cl^- or OH^-, in comparison to the synthesis in pure water or in solutions of non chlorinated salts or acids.[77,82,83] This is compatible with the increased density of surface charge in NMNp.[77,82,83] For example, in Fig. 11 we report some data about gold nanoparticles obtained by LASiS in water solutions of NaCl, with concentration variable between 0 and 10^{-1} M. The same experimental conditions (1064 nm (9 ns)–5 J cm^{-2}, 12 000 pulses)[60] were adopted for each solution. One can observe the increase of absorbance at the plasmon peak for increasing NaCl concentration until 10^{-2} M, while at 10^{-1} M NaCl the ablation yield is poor and the colloidal system becomes highly unstable. Similarly, the average size and the fraction of nonspherical AuNP decrease for increasing NaCl concentration until 10^{-2} M. These data are compatible with an increased surface charge of AuNP since the first stages of their formation. One can not exclude that ions influence the ablation mechanism other than the particles formation mechanism, although no indications about it can be found in literature.

For evaluating the stability of the AuNP solution we considered the percentage of absorbance decay at the plasmon peak after 5 days, denoted as $\Delta A(5)$. One can see that all solutions have $\Delta A(5)$ close to 0%, except for AuNP in the 10^{-1} M NaCl solution. Hence, below a concentration of 10^{-1} M, the presence of NaCl before LASiS did not affected particles stability.

These results definitively point out as the type and the concentration of electrolytes have relevant effects on NMNp obtained by LASiS.

Mafuné and co. intensely investigated the use of anionic surfactants like sodium dodecyl sulfate (SDS) for the LASiS of Pt, Au and Ag nanoparticles in water.[56,57,84] SDS revealed as an excellent ligand for obtaining NMNp solutions with long time stability. Mafuné and co. conjectured that anionic surfactants like SDS can be absorbed on particles surface through electrostatic interactions mediated by Na^+ ions, providing additional negative charges which stabilize NMNp.[76] On the contrary, cationic surfactants are inappropriate because they adsorb on particles surface, screening negative Au–O^- charges, with consequent particles aggregation.[76] Both Meunier and Mafuné groups concluded that adsorption of cationic or anionic surfactants are also mediated by the adsorption of their counter ions on NMNp surface.[76,77]

Mafuné and co. were able to reduce the standard deviation at about the 20–40% of the average radius by centrifugation of the NMNp solutions obtained by LASiS in presence of SDS.[56] They also found an inverse correlation between the concentration of SDS and the average particles size.[56,57] In fact, stabilizers compete with growth process like nuclei coalescence and adsorption of free atoms in solution by covering the surface of NMNp (Fig. 12).[57] The speed of surface coverage increase for increasing ligand concentration.[57]

Particles with small sizes have been obtained by LASiS of NMNp in presence of thiolated ligands (Table 2). The concentration of thiols is an effective parameter for the control of the average size of NMNp and the standard deviation is sensibly reduced with respect to LASiS in pure solvents. The size control mechanism is analogous to the case of SDS, but the effect is increased because of the larger sticking cross sections of thiols with respect to surfactants on particles surface.[57,73] The stability of the colloidal solution is improved by using thiolated molecules that are well solubilized in the ablation solvent.[65,73] The functionalization of NMNp coated with surfactants is not straightforward and this restricted the field of applications of this category of particles. In case of thiolated molecules, one can directly include the desired functional molecule or use thiols with easily manipolable chemical functionalities such as carboxilic groups. For instance, we previously reported the LASiS of AuNP coated with a fullerene derivative in dimethylsulfoxide for nonlinear optical applications[85] and with α-lipoic acid in acetonitrile.[65]

Interesting results in the size control of gold nanoparticles were obtained also by using cyclodextrins in water, which are supposed to coordinate AuNP by electrostatic interactions.[86]

4. Size manipulation by laser irradiation

At present, LASiS does not allow the predetermination of particles size and size distribution by varying few parameters

Table 2 NMNp obtained by LASiS in presence of solutes

Metal	*Solvent*	*Solutes*	*Size (Standard deviation)*	*Pulse wavelength (duration)-Fluence*	*Ref.*
Au	Water	SDS	6–12 nm (25–60%)	1064 nm (ns)–0.8 J cm^{-2}	57,86
	Water	PAMAM G5	3.5 nm (43%)	1064 nm (25 ps)	94
	Water	PAMAM G5	2.5 nm (20%)	532 nm (20 ps)	”
	Water	Cyclodextrins	2–16 nm (40–80%)	800 nm (120 fs)	77
	Decane	Dodecanethiol	2–5 nm	532 nm (5 ns) 0.5–30 J cm^{-2}	74
Ag	Water	SDS	16–8 nm (25–60%)	1064 nm (ns)	58
	Water	PVP	13–11 nm (50–80%)	1064 nm (ns)	Tsuji *et al.*; Appl. Surf. Sci. 2008, 5224
	Water	NaCl	26.4 nm (30%)	1064 nm (5 ns)	81
Pt	Water	SDS	3.0 nm (27%)	532 nm (ns)	Mafuné *et al.*; J. Phys. Chem. B 2003, 4218

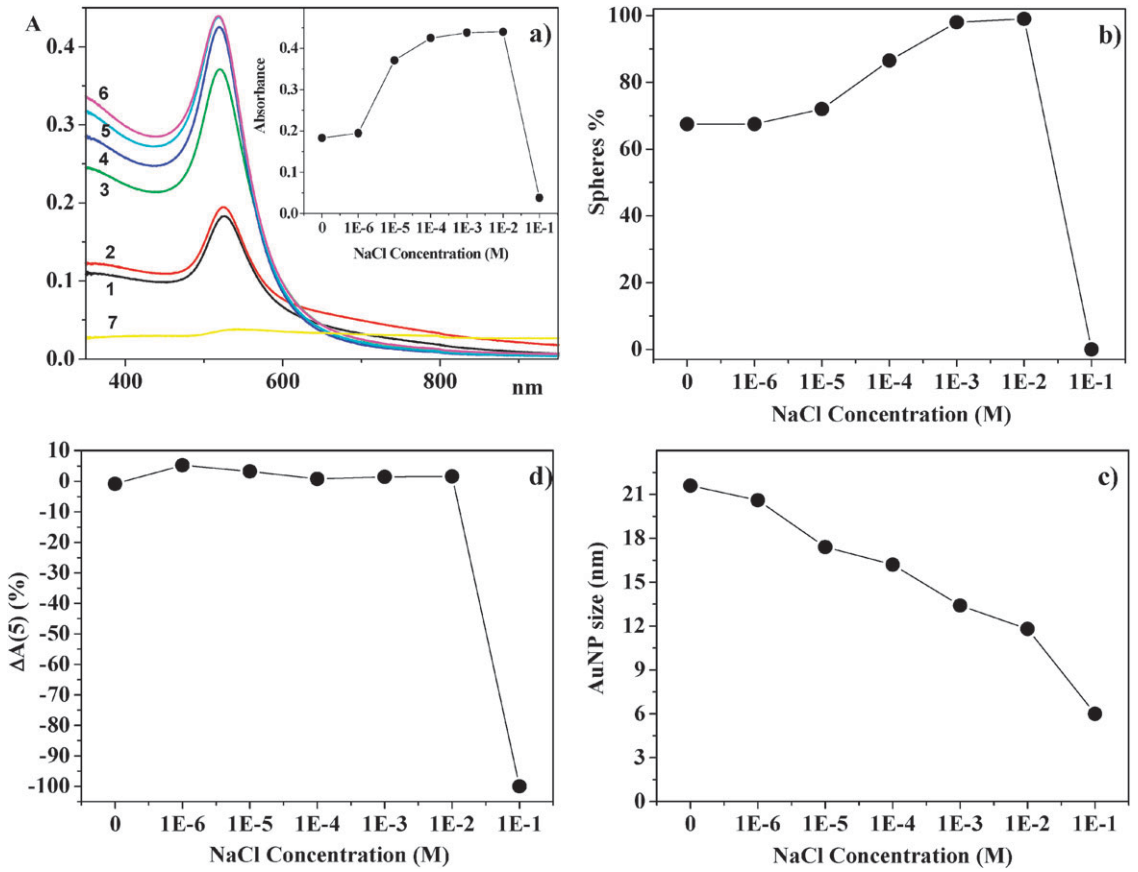

Fig. 11 LASiS of AuNP in water with increasing concentration of NaCl. (a) UV-visible spectra (2 mm optical path) corresponding to 0 M (1), 10^{-6} M (2), 10^{-5} M (3), 10^{-4} (4), 10^{-3} M (5), 10^{-2} M (6) and 10^{-1} M (7) NaCl. Inset shows the absorbance at the surface plasmon peak for all solutions. Figures (b) and (c) show the percentage of spherical nanoparticles and the average size as obtained by the MG fitting of the spectra in Fig. (a), according to ref. 28. (d) The absorbance difference in percentage at the surface plasmon peak after 5 days ΔA(5) for all solutions.

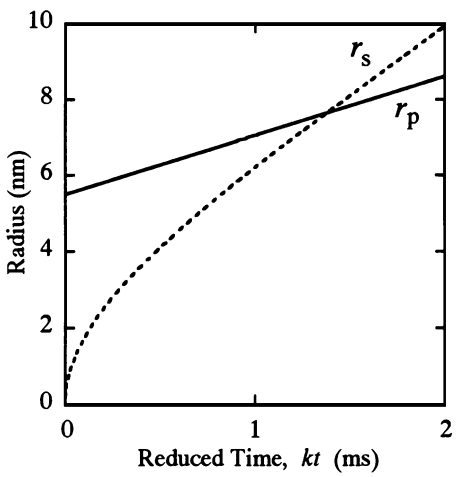

Fig. 12 Time evolution of the particle radius (r_p-solid line) and of the radius of particle entirely coated with SDS (r_s-dotted line), calculated on the basis of the dynamic formation model reported by Mafuné and co. When r_s cross r_p, particles growth is stopped. Reprinted with permission from ref. 58. Copyright (2000) American Chemical Society.

in a simple and controlled way, except when specific ligands are present in solution. However, laser irradiation methods which make possible the reduction or the increase of nanoparticles size, even in absence of stabilizing agents or other chemicals, have been developed. The size reduction method is based on fragmentation by photothermal heating of nanoparticles and can produce smaller nanoparticles of predetermined size with smaller standard deviation than the initial solution.[60,87–89] The size increase method is based on a two steps process, consisting of a controlled aggregation of nanoparticles and of the following laser irradiation of the solution to obtain photomelting of aggregates into larger nanoparticles.[60] Usually the size increase method requires centrifugation or other size selection techniques for obtaining standard deviations smaller than the initial solution, due to the low precision on the number of particles forming each aggregate.[60]

During laser irradiation, NMNp can absorb photons through plasmon excitations, interband transitions or multi-photon absorption processes, depending on pulse duration, wavelength and fluence.[54] Plasmon excitations are linear optical phenomena, prevailing at low fluence.[90] Interband transitions can be excited both through linear optical processes, for resonant laser wavelength, and through non-linear processes as simultaneous multiphoton absorption, in case of out of resonance laser wavelength.[90] Sequential multi-photon absorption processes are typical nonlinear optical phenomena, which prevails at high fluence, usually after

interband excitations. Simultaneous multiphoton absorptions are typical of femtosecond and picosecond pulses, while sequential multiphoton absorptions are typical of nanosecond laser pulses.

Pulse duration has important implications on the irradiation of NMNp. Femtosecond laser pulses are faster than the thermal relaxation processes, which means that their energy has not been transferred from electrons to the lattice at the end of the pulse.[54,90] Nanosecond and picosecond laser pulses have a time duration comparable with thermal relaxation processes, which means that part of the energy is released to the lattice as phonons or even to the solvent before the end of the pulse.[54,90] Moreover, the dephasing time of plasmon excitations is less than 10 fs, which implies that one femtosecond laser pulse can transfer a few tens of photons to each nanoparticle by plasmon absorption, while the remaining absorption processes consists in single electrons excitations.[54,90] During one nanosecond laser pulse, several thousands of photons can be absorbed by each metal nanoparticle through plasmon excitations, if the particle does not fragment for the whole pulse duration.[54,87,88,90] Hence the absorption of femtosecond pulses is weakly dependent on plasmon resonance, while nanosecond and picosecond pulses allow the selective heating of particles having plasmon bands in resonance with laser wavelengths.

Link and El Sayed performed two different irradiation experiments which are paradigmatic of the different response of NMNp to femtosecond and nanosecond laser pulses. In the first experiment, they irradiated a mixture of gold nanorods with different aspect ratios, *i.e.* different plasmon resonances, by 800 nm–250 mJ/cm^2 pulses of 100 fs and 7 ns, respectively.[54] In case of femtosecond pulses they obtained the complete reshaping of nanorods into nanospheres independent of the position of the plasmon resonance of nanorods. In case of nanosecond pulses, they obtained the selective reshaping into spheres of nanorods having a plasmon resonance peaked at 800 nm. Nanorods with moderate plasmon absorption at 800 nm were found partially reshaped into ϕ-like particles, while nanorods with low plasmon absorption at 800 nm were found unchanged at the end of the experiment.[54,90,91] This finding was attributed to heat dissipation contemporary to light absorption.[54] In the second experiment, Link and El Sayed increased the fluence of nanosecond laser pulses until obtaining a complete reshaping of all the nanorods in solution.[54,90,91] They found that, when nanorods with out-of-resonance plasmon absorptions were efficiently reshaped into spheres, in-resonance nanorods fragmented into smaller particles through a photoinduced explosive mechanism.[54,90,91] These findings evidenced that: (i) nanosecond irradiation can be selective on plasmon absorption, while femtosecond pulses are particularly suitable for plasmon-independent irradiation treatments; (ii) the absorption of nanosecond pulses can occur on a time-scale comparable with the rate of heat dissipation from particles to the environment.

Mafuné and co. thoroughly investigated the fragmentation of AuNP in aqueous SDS solutions irradiated with nanosecond laser pulses resonant with plasmon or interband excitations.[92–94] They found that nanoparticles fragment by coulomb explosion due to the sequential photoejection of electrons during the absorption of a single laser pulse.[94] By monitoring the presence of solvated electrons with pump and probe measurements, they found that the size of fragments decreased for increased number of photoejected electrons.[93] They also found that the rate of ionization was correlated to the absorption edge of interband transitions, which excluded thermoionic emission due to plasmon absorption as the ionization mechanism.[92]

Giorgetti and co. found that 532 nm picosecond laser irradiation of AuNP produced ionization and fragmentation through a two photon absorption process.[95] The energy of two photons at 532 nm (4.66 eV) is supposed to be very close to the ionizaton energy of one conduction electron in gold nanoparticles. Moreover, nonlinear optical phenomena like simultaneous two photon absorption are more probable with picosecond pulses at high fluence than with nanosecond pulses. However, experimental evidences suggest that particles ionization is the result of simultaneous particle heating and direct photoionization. For instance, Link and El Sayed found that heating of particles lattice after plasmon absorption has an important role in the successive photoionization and fragmentation.[54,90] The formation of Au^{3+} ions during the size reduction of AuNP solutions by 532 nm nanosecond and picosecond laser pulses was also reported, which is compatible with the formation of an high temperature gold plasma.[92,95,96] Finally, Plech and co. measured by time resolved X rays techniques that heating and melting precede fragmentation during irradiation with 800 nm–150 fs laser pulses of AuNP in water.[97,98]

Some authors suggested a different fragmentation mechanism, which supposes that particles can reach the vaporization threshold instead of coulomb explosion, if irradiated at moderate fluence.[88,89,99] In particular, Koda and co. measured by blackbody emission spectroscopy that gold nanoparticles irradiated by 7 ns–532 nm laser pulses at various fluences reached a temperature higher than the boiling threshold.[88,89] Fragmentation mechanisms involving heating with nanosecond laser pulses are sensible to particles size, because the rate of heat dissipation grows as R^{-2}, where R is the particles radius,[100] and is comparable to the heating rate at moderate fluences.[54] Moreover, due to surface dumping effects, plasmon absorption is weaker for smaller nanoparticles.[27,28] For instance, the absorption cross-section for unit volume at the plasmon peak of a 4 nm AuNP is about 4 times smaller than for a 30 nm AuNP.[28] In summary, the faster cooling rate and the slightly lower absorption rate of smaller nanoparticles are compatible with the selective fragmentation of larger nanoparticles during nanosecond laser irradiation with a fixed fluence.

Mafuné and co. investigated also the fate of AuNP fragments in presence or absence of stabilizers.[62,87,101–103] They found that fragments can coalesce forming spherical particles or, when present with high concentration, elongated fractal structures.[101–103] In presence of stabilizers, the average size of particles after fragmentation is reduced than in pure water, which confirmed that fragments are inclined to regrow.[101–103] According to these results, the minimum diameter is determined by the equilibrium between the efficiency of fragmentation and reaggregation.[101–103] For low aggregation efficiency, the minimum diameter can be reached by sequential

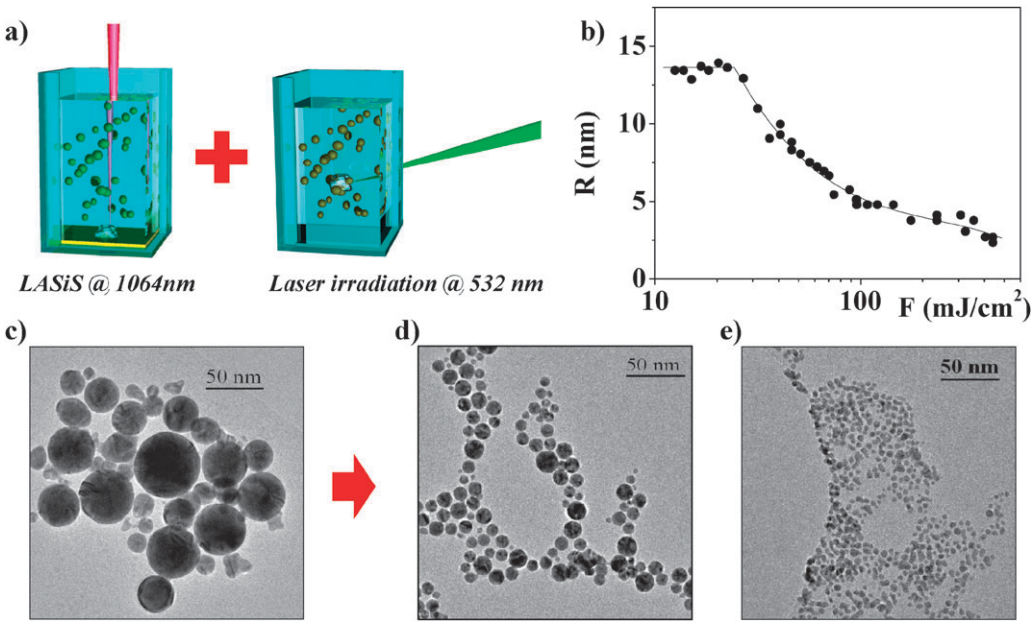

Fig. 13 (a) Cartoons sketching the size reduction of AuNP, consisting in the LASiS at 1064 nm and the following laser irradiation at 532 nm with a specific fluence. (b) Correlation between the average size of AuNP and the irradiation fluence at 532 nm. (c) Representative TEM images of AuNP as obtained by LASiS and after irradiation at 532 nm with 88 mJ cm^{-2} (d) and 442 mJ cm^{-2} (e). Adapted from ref. 61.

irradiation with more than one laser pulse. Size reduction of gold nanoparticles in presence of SDS produced particles smaller than 2 nm with about 20% of standard deviation.[87] Mafuné also plotted a structure diagram where the formation of isolated nanoparticles or fragments aggregation are reported as a function of laser fluence, AuNP concentration and SDS concentration.[103]

In a previous paper,[60] we reported the results of laser irradiation at 532 nm–9 ns of AuNP obtained by LASiS in pure water. We found that the average size of AuNP was progressively reduced by increasing laser fluence from 10 to 500 mJ/cm^2 (Fig. 13). Nanoparticles were stable in solution and their size distribution was monomodal, indicating the selective fragmentation of larger nanoparticles for increasing fluence, according to the fragmentation mechanisms discussed above. This point represents a critical difference with other experiments of the same type carried out by Mafuné,[87] Koda[88,89] or Inasawa,[99] where a bimodal size distribution after laser irradiation was reported due to the presence of ligands in solution. In our case, we were able to predetermine the AuNP size in a range between 25 and 4 nm by setting the appropriate fluence of the irradiation treatment. The standard deviation was progressively reduced from an initial value of about 60% (that of AuNP obtained by LASiS) to 20% for 4 nm particles, without the addition of any stabilizer, hence preserving the surface availability for further functionalization. The size reduction was successfully applied also to AuNP obtained by LASiS in organic solvents.[60]

NMNp obtained by LASiS in the absence of stabilizers often show a fraction of aggregated or nonspherical nanoparticles, as discussed in the previous sections.[28,65] Several authors studied reshaping of non spherical particles by laser irradiation in resonance with their plasmon absorption.[58,60,90,96] We exploited this mechanism for increasing the average size of nanoparticles by a two-step process (Fig. 14).[60] In the first step, we controlled the aggregation of AuNP obtained by LASiS in water by adding variable amounts of KCl and tetrahydrofuran (THF), in order to decrease the electric double layer thickness of the particles and to lower the dielectric constant of the solvent, respectively. Then, we irradiated the solutions at low fluence (1 mJ cm^{-2}) to reshape the aggregates into larger spheres. THF can be removed after the aggregation process by evaporation. We applied this method also to AuNP obtained by LASiS in organic solvents.[60]

Laser irradiation has often been used for the synthesis of alloy nanoparticles like Au–Ag, Au–Pd, Ag–Pd and Au–Pt.[104–107] The complete alloying was achieved in most cases, while sometimes only partial alloying was found, with the formation of inhomogeneous or core@shell structures.[107,108]

5. One step functionalization of NMNp

One of the main advantages of LASiS is the ability to obtain ligand-free NMNp in a variety of solvents. Therefore, functionalization with desired molecules can be obtained by choosing the solvent suitable for particle synthesis and molecule solubilization. Indeed, literature offers a few studies about functionalization of NMNp obtained by LASiS. Previously we reported the one-step functionalization of gold and silver nanoparticles obtained by LASiS in organic solvents with a variety of functional molecules like thermoresponsive polymers[109] or standard stabilizers as mercaptoethanol,[28] dodecanthiol or α-lipoic acid.[58] In the case of thiolated molecules which are soluble in organic solvents only, the one-step functionalization procedure represents a simplification with respect to CRMs, for the following reasons: (i) as discussed previously, most CRMs carried out in the presence of thiols allow the synthesis of NMNp with sizes of 2–5 nm,[2]

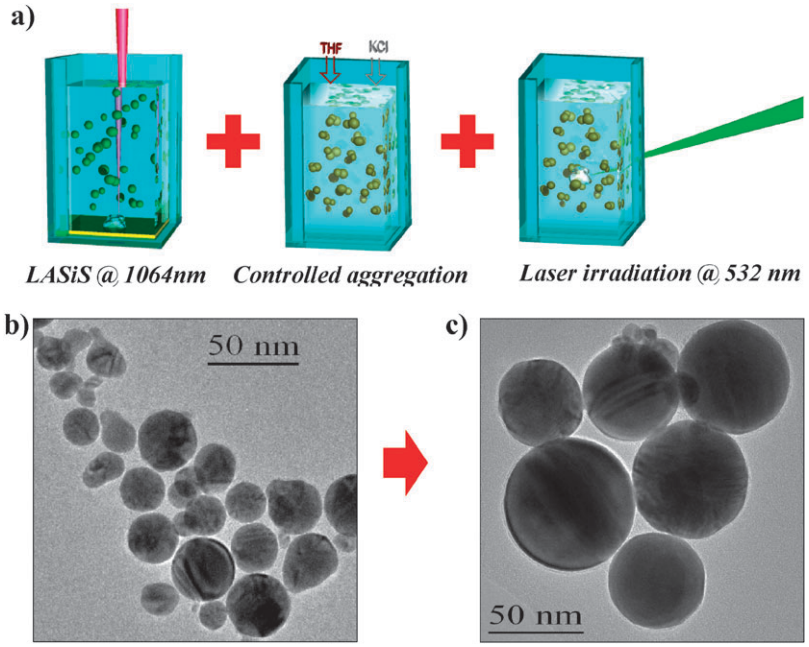

Fig. 14 (a) Cartoons sketching the size increase of AuNP, consisting in the LASiS at 1064 nm, the controlled aggregation of nanoparticles by addition of THF and KCl and photomelting by laser irradiation at 532 nm. (b) Representative TEM images of AuNP as obtained by LASiS and after the size increase treatment (c). From ref. 61.

which show a poor plasmonic response; NMNp with a larger size can be obtained by LASiS in pure organic solvents and functionalized later, as done in our previous works;[28,60,65] (ii) more than a single type of thiols can be added to the same solution of NMNp obtained by LASiS, without affecting their size and plasmonic properties; (iii) different types of thiols can be added to different solutions containing the same NMNp, hence one can obtain the same NMNp covered with different thiols, as was done in our previous works about AgNP[58] and AuNP (Fig. 15).[28]

However, surface contamination of NMNp obtained in pure organic solvents needs to be carefully evaluated, as specific studies about this problems are limited.

We also demonstrated that the surface of AuNP obtained by LASiS in water is highly accessible for bioconjugation and is suitable for UV-visible monitoring of surface coverage.[58,60] In our experiment, we added increasing amounts of bovine serum albumine (BSA) to a solution of 8 nm AuNP, obtained by LASiS and size reduction in pure water (Fig. 16).[60] By monitoring the red shift and the absorbance change after the addition of increasing amounts of BSA, we obtained the sigmoidal curves reported in Fig. 16. These curves give clear indications of the progressive surface coverage of particles with BSA. We measured a red shift and an absorbance change of the plasmon band for a ratio of BSA to AuNP as low as 1 : 10. In the case of a solution of 30 nm nanoparticles, we measured the changes in the plasmon band above a BSA : AuNP ratio of about 100 : 1.[60]

In our previous work about AuNP surface coating with the thermoresponsive thiol terminated poly-*N*-isopropylacrylamide-co-acrylamide co-polymer,[109] we used the red-shift of surface plasmon absorption for estimating the polymer amount required for nanoparticle surface saturation. The

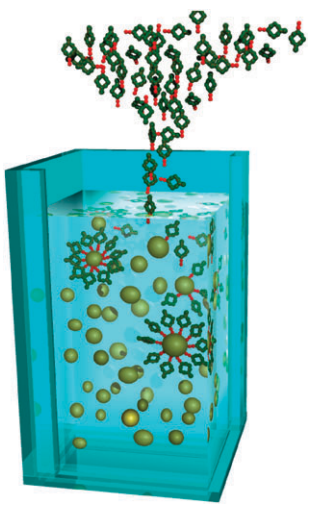

Fig. 15 Cartoon reporting an important advantage of NMNp obtained by LASiS: one-step functionalization by addition of the desired molecules in solution of ligand-free nanoparticles.

number of polymer chains for each AuNP was evaluated by the same measurements. In particular, we measured the red-shift of the surface plasmon absorption for a ratio of thiolated polymer : AuNP varying from 310 : 1 to 61 300 : 1 and we found surface saturation for a ratio of about 4000 : 1 (average AuNP size of 18 nm). These figures were in fair agreement with simultaneous iodine titration measurements on the unbound polymer obtained after centrifugation of the AuNP–polymer solution.[109]

The use of this type of plots for the real time monitoring with high sensitivity of nanoparticles the multi-functionalization is promising. Once the saturation concentration has been

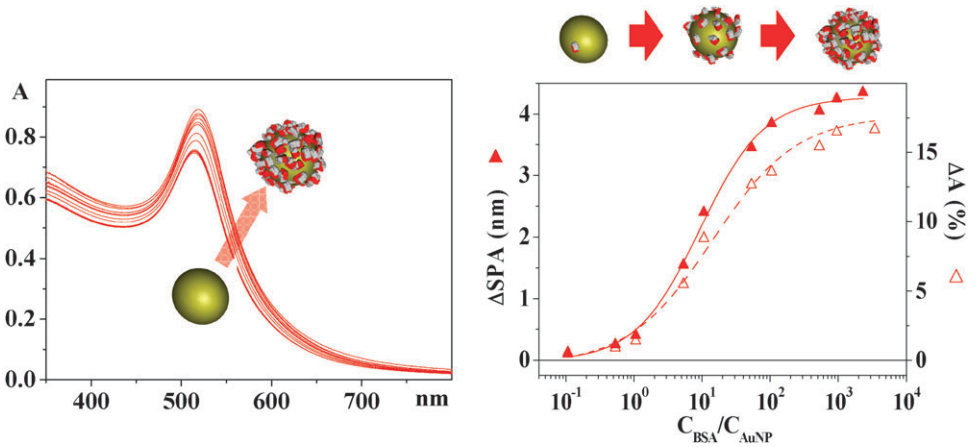

Fig. 16 Left: real time monitoring by UV-visible spectroscopy of the evolution of the surface plasmon band of AuNP obtained by LASiS in water by addition of increasing amounts of BSA. Right: the red shift of the surface plasmon absorption (ΔSPA) and the percentage differential absorption (ΔA) *versus* the BSA : AuNP ratio. From ref. 61.

estimated by separate experiments for each ligand type, the sequential addition of ligands with the desired ratio is facilitated. Such procedure can be important whenever ligands are scarce or precious, as often happens in the case of NMNp bioconjugation, because the saturation concentration can be measured in a brief time and on volumes as small as those required for a UV-visible analysis.

We also observed a very good stability for AuNP and AgNP solutions during the addition of ligands, *i.e.* no aggregation.[28,58,60] This finding is compatible with the strong adhesion of stabilizing charges (for instance, the Au–O^- groups) on the surface of NMNp obtained by LASiS, contrary to the case of citrate stabilized NMNp.

However, some important aspects of the surface functionalization of NMNp obtained by LASiS in pure solvents or in the presence of ligands have not been studied to date. For instance, it is unknown if thiols can form compact monolayers on the surface of NMNp obtained by LASiS, or if the presence of a partial oxidation induces different ligand morphologies. Also, the role of solvent pyrolysis on particles functionalization has not been elucidated.

6. Conclusions

LASiS and laser irradiation methods for size manipulation can meet the increasing demand for NMNp in science and applied technology. LASiS is a physical approach for the top–down synthesis of nanomaterials, complementary to bottom–up chemical reduction methods. We can summarize the main peculiarities of LASiS as following:

— the experimental set up is essential and the start-up costs can be of the order of 15–20 keuro, laser included;

— metal plates required for the synthesis are less expensive than metal salts and other chemicals required by CRMs;

— LASiS is a "green" technique and has good reproducibility;

— NMNp can be obtained without any ligands or stabilizers in a variety of solvents, which allows one-step functionalization;

— UV-visible spectroscopy of the plasmon bands can be used for monitoring the surface coverage of NMNp, which is particularly useful for obtaining multifunctionalization;

— LASiS can be used as a unitary approach for the synthesis of NMNp of different metals, in different solvents, with different surface functionalization, conversely to the plethora of chemical reduction methods;

— it is a promising technique also for the synthesis of other materials like semiconductor, magnetic or organic nanoparticles and of metastable phases.

However, LASiS still has some important drawbacks, when compared to traditional CRMs, namely:

— the control on the average size and size distribution is limited;

— the synthesis in organic solvents can produce pyrolysis of organic molecules with consequent contamination of NMNp surface;

— the mass production of NMNp by LASiS is possible only by high repetition rate lasers.

In this perspective article we also evidenced that many unexplored issues exist about LASiS, which have fundamental implications on the synthesis results:

— the ablation mechanism is still not completely understood, which explains the low control on particle size distribution and structure;

— the effect of solvents and solutes on the control of particle structure and composition has been considered only in few cases;

— the surface chemistry of NMNp obtained in water and organic solvents is poorly controlled and in some cases completely unknown;

— the implications of particle surface chemistry on their stability and functionalization is quite unknown in most cases.

The interesting results obtained by LASiS of NMNp until now suggest that this technique can represent a fertile field for further investigations and could prove an indispensable approach for the synthesis of nanomaterials in the future.

Acknowledgements

V.A. acknowledges financial support from University of Padova (Assegno di Ricerca n. 177-2008).

References

1 Y. Xia and N. J. Halas, *MRS Bull.*, 2005, **30**, 338–348.
2 M. C. Daniel and D. Astruc, *Chem. Rev.*, 2004, **104**, 293–346.
3 P. G. Etchegoin and E. C. L. Ru, *Phys. Chem. Chem. Phys.*, 2008, **10**, 6079–6089.
4 C. J. Murphy, A. M. Gole, J. W. Stone, P. N. Sisco, A. M. Alkilany, E. C. Goldsmith and S. C. Baxter, *Acc. Chem. Res.*, 2008, **41**, 1721–1730.
5 A. Caragheorgheopol and V. Chechik, *Phys. Chem. Chem. Phys.*, 2008, **10**, 5029–5041.
6 A. Corma and H. Garcia, *Chem. Soc. Rev.*, 2008, **37**, 2096–2126.
7 N. L. Rosi and C. A. Mirkin, *Chem. Rev.*, 2005, **105**, 1547–1562.
8 M. Ferrari, *Nat. Rev. Cancer.*, 2005, **5**, 161–171.
9 I. Hussain, S. Graham, Z. Wang, B. Tan, D. C. Sherrington, S. P. Rannard, A. I. Cooper and M. Brust, *J. Am. Chem. Soc.*, 2005, **127**, 16398–16399.
10 C. J. Ackerson, P. D. Jadzinsky, G. J. Jensen and R. D. Kornberg, *J. Am. Chem. Soc.*, 2006, **128**, 2635–2640.
11 J. Shan and H. Tenhu, *Chem. Commun.*, 2007, **2007**, 4580–4598.
12 A. C. Templeton, W. P. Wuelfing and R. W. Murray, *Acc. Chem. Res.*, 2000, **33**, 27–36.
13 J. M. Abad, S. F. L. Mertens, M. Pita, V. M. Fernandez and D. J. Schiffrin, *J. Am. Chem. Soc.*, 2005, **127**, 5689–5694.
14 M. Brust, J. Fink, D. Bethell, D. J. Schiffrin and C. Kiely, *Chem. Commun.*, 1995, **1995**, 1655–1656.
15 A. G. Tkachenko, H. Xie, Y. Liu, D. Coleman, J. Ryan, W. R. Glomm, M. K. Shipton, S. Franzen and D. L. Feldheim, *Bioconjug. Chem.*, 2004, **15**, 482–490.
16 R. Shukla, S. K. Nune, N. Chanda, K. Katti, S. Mekapothula, R. R. Kulkarni, W. V. Welshons, R. Kannan and K. V. Katti, *Small*, 2008, **4**, 1425–1436.
17 M. G. Bellino, E. J. Calvo and G. Gordillo, *Phys. Chem. Chem. Phys.*, 2004, **6**, 424–428.
18 C. Doty, D. J. Schiffrin, R. J. Nichols, N. T. K. Thanh, I. Hussain, M. Brust, D. G. Fernig and R. Lévy, *J. Am. Chem. Soc.*, 2004, **126**, 10076.
19 S. H. Brewer, W. R. Glomm, M. C. Johnson, M. K. Knag and S. Franzen, *Langmuir*, 2005, **21**, 9303–9307.
20 N. Pernodet, X. Fang, Y. Sun, A. Bakhtina, A. Ramakrishnan, J. Sokolov, A. Ulman and M. Rafailovich, *Small*, 2006, **2**, 766.
21 C. M. Goodman, C. D. McCusker, T. Yilmaz and V. M. Rotello, *Bioconjug. Chem.*, 2004, **15**, 897–900.
22 M. E. Aubin-Tam and K. Hamad-Schifferli, *Biomed. Mater.*, 2008, **3**, 17.
23 R. Munday, *FreeRadic. Biol. Med.*, 1989, **7**, 659–673.
24 G. Merga, L. C. Cass, D. M. Chipman and D. Meisel, *J. Am. Chem. Soc.*, 2008, **130**, 7067–7076.
25 D. Steiner, T. Mokari, U. Banin and O. Millo, *Phys. Rev. Lett.*, 2005, **95**, 56805.
26 H. Peisert, A. Petershans and T. Chasse, *J. Phys. Chem. C*, 2008, **112**, 5703–5706.
27 U. Kreibig and M. Vollmer, *Optical Properties of Metal Clusters*, Springer, Heidelberg, 1995.
28 V. Amendola and M. Meneghetti, *J. Phys. Chem. C*, 2009, **113**, 4277–4285.
29 C. J. Murphy, *J. Mater. Chem.*, 2008, **18**, 2173–2176.
30 C. A. Waters, A. J. Mills, K. A. Johnson and D. J. Schiffrin, *Chem. Commun.*, 2003, **2003**, 540–541.
31 Y. P. Sun and J. E. Riggs, *Int. Rev. Phys. Chem.*, 1999, **18**, 43–90.
32 S. F. Sweeney, G. H. Woehrle and J. E. Hutchison, *J. Am. Chem. Soc.*, 2006, **128**, 3190–3197.
33 P. Raveendran, J. Fu and S. L. Wallen, *Green Chem.*, 2006, **8**, 34–38.
34 P. Raveendran, J. Fu and S. L. Wallen, *J. Am. Chem. Soc.*, 2003, **125**, 13940–13941.
35 M. N. Nadagouda and R. S. Varma, *Green Chem.*, 2008, **10**, 859–862.
36 B. Hu, S. Wang, K. Wang, M. Zhang and S. Yu, *J. Phys. Chem. C*, 2008, **112**, 11169–11174.
37 K. L. McGilvray, M. R. Decan, D. Wang and J. C. Scaiano, *J. Am. Chem. Soc.*, 2006, **128**, 15980–15981.
38 J. Liu, G. Qin, P. Raveendran and Y. Ikushima, *Chem.–Eur. J.*, 2006, **12**, 2131.
39 C. Phipps, *Laser Ablation and its Applications*, Springer, Heidelberg, 2007.
40 A. Fojtik and A. Henglein, *Ber. Bunsen-Ges. Phys. Chem.*, 1993, **97**, 252–254.
41 H. Cui, P. Liu and G. W. Yang, *Appl. Phys. Lett.*, 2006, **89**, 153124.
42 K. Saitow, T. Yamamura and T. Minami, *J. Phys. Chem. C*, 2008, **112**, 18340–18349.
43 C. Momma, B. N. Chichkov, S. Nolte, F. von Alvensleben, A. Tünnermann, H. Welling and B. Wellegehausen, *Opt. Commun.*, 1996, **129**, 134–142.
44 L. V. Zhigilei, P. B. S. Kodali and B. J. Garrison, *J. Phys. Chem. B*, 1998, **102**, 2845–2853.
45 G. W. Yang, *Prog. Mater. Sci.*, 2007, **52**, 648–698.
46 R. Fabbro, J. Fournier, P. Ballard, D. Devaux and J. Virmont, *J. Appl. Phys.*, 1990, **68**, 775.
47 T. Sakka, S. Iwanaga, Y. H. Ogata, A. Matsunawa and T. Takemoto, *J. Chem. Phys.*, 2000, **112**, 8645.
48 T. Tsuji, Y. Okazaki, Y. Tsuboi and M. Tsuji, *Jpn. J. Appl. Phys.*, 2007, **46**, 1533–1535.
49 J. P. Sylvestre, A. V. Kabashin, E. Sacher and M. Meunier, *Appl. Phys. A*, 2005, **80**, 753–758.
50 W. T. Nichols, T. Sasaki and N. Koshizaki, *J. Appl. Phys.*, 2006, **100**, 114911.
51 W. T. Nichols, T. Sasaki and N. Koshizaki, *J. Appl. Phys.*, 2006, **100**, 114912.
52 R. Knochenmuss, *Analyst*, 2006, **131**, 966–986.
53 A. V. Kabashin and M. Meunier, *J. Appl. Phys.*, 2003, **94**, 7941.
54 S. Link and M. A. El-Sayed, *Int. Rev. Phys. Chem.*, 2000, **19**, 409–453.
55 T. Asahi, T. Sugiyama and H. Masuhara, *Acc. Chem. Res.*, 2008, **41**, 1790–1798.
56 F. Mafune, J. Kohno, Y. Takeda, T. Kondow and H. Sawabe, *J. Phys. Chem. B*, 2001, **105**, 5114–5120.
57 F. Mafune, J. Kohno, Y. Takeda, T. Kondow and H. Sawabe, *J. Phys. Chem. B*, 2000, **104**, 9111–9117.
58 V. Amendola, S. Polizzi and M. Meneghetti, *Langmuir*, 2007, **23**, 6766–6770.
59 G. Compagnini, A. A. Scalisi and O. Puglisi, *J. Appl. Phys.*, 2003, **94**, 7874.
60 V. Amendola and M. Meneghetti, *J. Mater. Chem.*, 2007, **17**, 4705–4710.
61 G. Compagnini, A. A. Scalisi and O. Puglisi, *Phys. Chem. Chem. Phys.*, 2002, **4**, 2787–2791.
62 F. Mafuné and T. Kondow, *Chem. Phys. Lett.*, 2004, **383**, 343–347.
63 W. T. Nichols, T. Sasaki and N. Koshizaki, *J. Appl. Phys.*, 2006, **100**, 114913.
64 T. Tsuji, T. Kakita and M. Tsuji, *Appl. Surf. Sci.*, 2003, **206**, 314–320.
65 V. Amendola, S. Polizzi and M. Meneghetti, *J. Phys. Chem. B*, 2006, **110**, 7232–7237.
66 K. Anikin, N. Melnik, A. Simakin, G. Shafeev, V. Voronov and A. Vitukhnovsky, *Chem. Phys. Lett.*, 2002, **366**, 357–360.
67 H. Zeng, W. Cai, J. Hu, G. Duan, P. Liu and Y. Li, *Appl. Phys. Lett.*, 2006, **88**, 171910.
68 K. Saitow, *J. Phys. Chem. B*, 2005, **109**, 3731–3733.
69 C. Liang, Y. Shimizu, M. Masuda, T. Sasaki and N. Koshizaki, *Chem. Mater.*, 2004, **16**, 963–965.
70 P. Liu, W. Cai and H. Zeng, *J. Phys. Chem. C*, 2008, **112**, 3261–3266.
71 M. Nath, C. N. R. Rao, R. Popovitz-Biro, A. Albu-Yaron and R. Tenne, *Chem. Mater.*, 2004, **16**, 2238–2243.
72 G. X. Chen, M. H. Hong, B. Lan, Z. B. Wang, Y. F. Lu and T. C. Chong, *Appl. Surf. Sci.*, 2004, **228**, 169–175.
73 G. Compagnini, A. A. Scalisi, O. Puglisi and C. Spinella, *J. Mater. Res.*, 2004, **19**, 2795–2798.
74 T. Tsuji, K. Iryo, N. Watanabe and M. Tsuji, *Appl. Surf. Sci.*, 2002, **202**, 80–85.
75 V. Amendola, G. A. Rizzi, S. Polizzi and M. Meneghetti, *J. Phys. Chem. B*, 2005, **109**, 23125–23128.
76 H. Muto, K. Yamada, K. Miyajima and F. Mafune, *J. Phys. Chem. C*, 2007, **111**, 17221–17226.
77 J. P. Sylvestre, S. Poulin, A. V. Kabashin, E. Sacher, M. Meunier and J. H. T. Luong, *J. Phys. Chem. B*, 2004, **108**, 16864–16869.

78 L. K. Ono and B. Roldan Cuenya, *J. Phys. Chem. C*, 2008, **112**, 4676–4686.
79 R. M. Tilaki, A. Iraji zad and S. M. Mahdavi, *Appl. Phys. A*, 2007, **88**, 415–419.
80 T. Tsuji, K. Iryo, Y. Nishimura and M. Tsuji, *J. Photochem. Photobiol. A*, 2001, **145**, 201–207.
81 M. S. Yeh, Y. S. Yang, Y. P. Lee, H. F. Lee, Y. H. Yeh and C. S. Yeh, *J. Phys. Chem. B*, 1999, **103**, 6851–6857.
82 C. H. Bae, S. H. Nam and S. M. Park, *Appl. Surf. Sci.*, 2002, **197**, 628–634.
83 K. Siskova, B. Vlckova, P. Y. Turpin and C. Fayet, *J. Phys. Chem. C*, 2008, **112**, 4435–4443.
84 F. Mafuné and T. Kondow, *Chem. Phys. Lett.*, 2003, **372**, 199–204.
85 V. Amendola, G. Mattei, C. Cusan, M. Prato and M. Meneghetti, *Synth. Met.*, 2005, **155**, 283–286.
86 J. P. Sylvestre, A. V. Kabashin, E. Sacher, M. Meunier and J. H. Luong, *J. Am. Chem. Soc.*, 2004, **126**, 7176–7177.
87 F. Mafune, J. Kohno, Y. Takeda and T. Kondow, *J. Phys. Chem. B*, 2002, **106**, 7575–7577.
88 A. Takami, H. Kurita and S. Koda, *J. Phys. Chem. B*, 1999, **103**, 1226–1232.
89 H. Kurita, A. Takami and S. Koda, *Appl. Phys. Lett.*, 1998, **72**, 789.
90 S. Link and M. A. El-Sayed, *Ann. Rev. Phys. Chem.*, 2003, **54**, 331–366.
91 S. Link, C. Burda, B. Nikoobakht and M. A. El-Sayed, *J. Phys. Chem. B*, 2000, **104**, 6152–6163.
92 M. Shoji, K. Miyajima and F. Mafune, *J. Phys. Chem. C*, 2008, **112**, 1929–1932.
93 K. Yamada, K. Miyajima and F. Mafuné, *J. Phys. Chem. C*, 2007, **111**, 11246–11251.
94 K. Yamada, Y. Tokumoto, T. Nagata and F. Mafune, *J. Phys. Chem. B*, 2006, **110**, 11751.
95 A. Giusti, E. Giorgetti, S. Laza, P. Marsili and F. Giammanco, *J. Phys. Chem. C*, 2007, **111**, 14984–14991.
96 T. E. McGrath, A. C. Beveridge and G. J. Diebold, *Angew. Chem.*, 1999, **38**, 3353–3356.
97 A. Plech, V. Kotaidis, S. Grésillon, C. Dahmen and G. von Plessen, *Phys. Rev. B*, 2004, **70**, 195423.
98 A. Plech, V. Kotaidis, M. Lorenc and M. Wulff, *Chem. Phys. Lett.*, 2005, **401**, 565–569.
99 S. Inasawa, M. Sugiyama, S. Noda and Y. Yamaguchi, *J. Phys. Chem. B*, 2006, **110**, 3114.
100 M. Hu and G. V. Hartland, *J. Phys. Chem. B*, 2002, **106**, 7029–7033.
101 N. Matsuo, H. Muto, K. Miyajima and F. Mafuné, *Phys. Chem. Chem. Phys.*, 2007, **9**, 6027–6031.
102 F. Mafune, J. Kohno, Y. Takeda and T. Kondow, *J. Phys. Chem. B*, 2001, **105**, 9050–9056.
103 F. Mafuné, *Chem. Phys. Lett.*, 2004, **397**, 133–137.
104 G. Compagnini, E. Messina, O. Puglisi and V. Nicolosi, *Appl. Surf. Sci.*, 2007, **254**, 1007–1011.
105 Y. H. Chen, Y. H. Tseng and C. S. Yeh, *J. Mater. Chem.*, 2002, **12**, 1419–1422.
106 D. B. Pedersen, S. Wang, E. J. S. Duncan and S. H. Liang, *J. Phys. Chem. C*, 2007, **111**, 13665–13672.
107 F. Mafune, J. Kohno, Y. Takeda and T. Kondow, *J. Am. Chem. Soc.*, 2003, **125**, 1686–1687.
108 G. Compagnini, E. Messina, O. Puglisi, R. S. Cataliotti and V. Nicolosi, *Chem. Phys. Lett.*, 2008, **457**, 386–390.
109 S. Salmaso, P. Caliceti, V. Amendola, M. Meneghetti, J. P. Magnusson, G. Pasparakis and C. Alexander, *J. Mater. Chem.*, 2009, **19**, 1608–1615.